Mathematical Biosciences and Engineering

MBE, 20(8): 14306–14326.
DOI: 10.3934/mbe.2023640
Received: 10 October 2022
Revised: 10 June 2023
Accepted: 15 June 2023
Published: 29 June 2023

http://www.aimspress.com/journal/MBE

Research article

Deep reinforcement learning framework for controlling infectious disease outbreaks in the context of multi-jurisdictions

Seyedeh Nazanin Khatami[1,*] and Chaitra Gopalappa[2]

[1] MGH Institute for Technology Assessment, Harvard Medical School, Boston, MA 02114, USA
[2] Mechanical and Industrial Engineering Department, University of Massachusetts Amherst, Amherst, MA 01003, USA

* **Correspondence:** Email: skhatami@mgh.harvard.edu.

Abstract: In the absence of pharmaceutical interventions, social distancing and lockdown have been key options for controlling new or reemerging respiratory infectious disease outbreaks. The timely implementation of these interventions is vital for effectively controlling and safeguarding the economy.Motivated by the COVID-19 pandemic, we evaluated whether, when, and to what level lockdowns are necessary to minimize epidemic and economic burdens of new disease outbreaks. We formulated the question as a sequential decision-making Markov Decision Process and solved it using deep Q-network algorithm. We evaluated the question under two objective functions: a 2-objective function to minimize economic burden and hospital capacity violations, suitable for diseases with severe health risks but with minimal death, and a 3-objective function that additionally minimizes the number of deaths, suitable for diseases that have high risk of mortality.A key feature of the model is that we evaluated the above questions in the context of two-geographical jurisdictions that interact through travel but make autonomous and independent decisions, evaluating under cross-jurisdictional cooperation and non-cooperation. In the 2-objective function under cross-jurisdictional cooperation, the optimal policy was to aim for shutdowns at 50 and 25% per day. Though this policy avoided hospital capacity violations, the shutdowns extended until a large proportion of the population reached herd immunity. Delays in initiating this optimal policy or non-cooperation from an outside jurisdiction required shutdowns at a higher level of 75% per day, thus adding to economic burdens. In the 3-objective function, the optimal policy under cross-jurisdictional cooperation was to aim for shutdowns of up to 75% per day to prevent deaths by reducing infected cases. This optimal policy continued for the entire duration of the simulation, suggesting that, until pharmaceutical interventions such as treatment or vaccines become available, contact reductions through physical distancing would be necessary to minimize deaths. Deviating from this policy increased the number of shutdowns and led to several deaths.In summary, we present a decision-analytic methodology for identifying optimal lockdown strategy under the context of interactions between jurisdictions that make autonomous and independent decisions. The numerical analysis outcomes are intuitive and, as expected, serve as proof

of the feasibility of such a model. Our sensitivity analysis demonstrates that the optimal policy exhibits robustness to minor alterations in the transmission rate, yet shows sensitivity to more substantial deviations. This finding underscores the dynamic nature of epidemic parameters, thereby emphasizing the necessity for models trained across a diverse range of values to ensure effective policy-making.

Keywords: decision-making in epidemics; COVID-19; deep reinforcement learning; artificial intelligence in public health; non-pharmaceutical intervention; jurisdictional decision-making

1. Introduction

Timely implementations of pharmaceutical and non-pharmaceutical interventions (NPI) are critical for effective control of new infectious disease outbreaks. Delay in response causes enormous disease and economic burdens, as seen during the COVID-19 outbreak caused by the SARS-Cov2 virus [1].

In the event of new respiratory infectious disease outbreaks, when pharmaceutical interventions are unavailable, NPIs are the only options, as was the case with COVID-19. Effective NPI options include facemask-use and social distancing [2]. Social distancing could include physical distancing (e.g., by 3 ft or 6 ft) or partial lockdowns. While facemasks and physical distancing could be the most economically feasible options, lockdowns may be necessary for highly contagious viruses such as the SARS-Cov2. While locking-down early in the pandemic would be suitable for reducing disease burden, it may unnecessarily add to the economic burden. On the other hand, delaying the lockdown or improper phasing of lockdowns can significantly amplify both economic and disease burdens [3].

In this context, through timely implementation of lockdowns, governmental public health agencies play a key role in effective containment of new outbreaks. Furthermore, though public health decisions are autonomous to each jurisdiction, e.g., in the United States, local COVID-19 prevention guidelines were determined by individual states [4], the epidemic can be influenced by outside jurisdictions through travel.

The objective of our work is to a) Propose a reinforcement learning (RL) model designed specifically for the sequential analyses of epidemic decisions. b) Investigate jurisdiction-specific decisions within the context of multi-jurisdictional interactions, and subsequently conduct numerical analyses that aim to demonstrate the significance of these jurisdictional interactions.

A methodology that can help determine whether and when a lockdown is necessary, to what level, and how to phase out a lockdown would be a critical part of a pandemic preparedness plan. While surveillance systems to help identify new outbreaks would be a crucial part of this preparedness plan, because of the delay in diagnosis of cases, informing decisions only based on data collected through these systems will not be sufficient. Surveillance data combined with epidemic projections through the use of dynamic mathematical models can help identify optimal control policies, including whether a partial shutdown will be necessary [4,5]. In this study, we formulated the question of whether and when a lockdown is necessary, to what level, and how to phase out a lockdown as a sequential decision-making problem using Markov decision process (MDP) and solved using Deep Q-network (DQN), a reinforcement learning (RL) algorithm.

Reinforcement Learning (RL) is a branch of Artificial Intelligence (AI) where optimal policies are learned through a trial-and-error learning process. This iterative cycle involves an agent taking action (e.g., intervention decision) based on the system's current state, causing a transition to a subsequent state associated with a given reward [6], and as the number of iterations increase it learns to take decisions with the highest reward, continuing until the algorithm has converged to the optimal

decision. Research in RL algorithms can be broadly categorized into three areas: the formulation of the decision analytic algorithm as a RL problem, an algorithm for learning these decisions, and the data required to train the algorithm. The focus of this work is solely on the first component: the formulation of the decision analytic algorithm.

For the second component, algorithms for learning decisions, several algorithms are available in the current literature. For our purpose, we utilized the Deep Q-Network (DQN), an off-the-shelf RL algorithm, for its capacity to handle extensive environments pertinent to COVID-19 modeling [5]. DQN has been employed across a broad spectrum of problems. This includes, but is not limited to, applications such as games [7], autonomous driving [8], recommendation system [9], mobile robot navigation [10], computer-aided diagnosis [11], stock trading [12], and very recently on COVID-19 pandemic control [13,14].

For the third component, in application of RL to disease epidemics, simulation models are widely used to generate the data to train the algorithms [15]. There are two broad categorizations of simulation models, agent-based and compartmental models that are typically employed. Generally, compartmental models are apt for rapidly spreading diseases and allow for heterogeneity by partitioning compartments. Alternatively, agent-based models are often more suitable for slower spreading diseases, where contact structures play a significant role. In this work, as our focus was not on the simulation model itself, we utilized a simple compartmental model (i.e., with no heterogeneity in demographics), but any simulation environment could be substituted depending on the nature of disease spread and research question.

As noted above, our focus is on the first component, formulation of decision analytic algorithm (here COVID-related interventions) as a RL problem. The recent literature has seen an influx of RL models related to this focus. There are three components to this model formulation: the state space, the action (intervention) space, and the reward function. Amid the COVID-19 pandemic, lockdowns have become a primary intervention to curb disease spread. Consequently, an increasing number of RL studies formulated the problem as identifying optimal lockdown policies with the objective of minimizing COVID-19 cases while also mitigating economic damages. For instance, Khadilkar et al. harnessed RL to automate policy learning, thereby optimizing lockdown policies for epidemic control [16]. They denoted their state space as different components of the compartmental model, the action space as lockdown or no lockdown, and the reward function as the negative of the number of deaths, persons infected, and the number of days with lockdown. Similarly, Kompella et al. [17] devised an agent-based pandemic simulator and an RL-based methodology to optimize fine-grained mitigation policies that minimize economic impact without overtaxing hospital capacity. They formulated their state space as the number of people within each infection state, the action space as different stages of lockdown, and the reward function as a combination of increasing economy while minimizing capacity violation. Further, Arango et al. employed RL to optimize cyclic lockdowns as a temporary alternative to extended lockdowns, aiming to minimize ICU usage overshoots and lockdown duration for socio-economic benefit [18]. They formulated their RL components as follows: the state space being the current number of infected persons, the action space being either non-lockdown or lockdown, and the reward function as a combination of the economy and the number of available ICU beds.

As with our case, these studies utilized off-the-shelf learning algorithms and constructed simulation models (either compartmental or agent-based) for training. Their contributions primarily lie in 'formulating the epidemic decision analytic problem' as an RL problem. Our model contributes to this existing body of work. A gap in these literature models is that they overlook cross-jurisdictional interactions. We address this gap through novel formulation of the state space to consider jurisdictional interactions.

We present an RL model trained using the DQN algorithm to evaluate the question of whether a lockdown is necessary, and if so, when it should be initiated, to what level (proportion lockdown), and how it should change over time, such that it minimizes both epidemic and economic burdens. Though this objective is similar to other RL studies in the literature, our work differs from previous work in two ways. First, we evaluated the question of when to initiate a lockdown policy, which would be helpful for future outbreaks of similar epidemiology when lockdowns are a key intervention. Second, we evaluate these decisions in the context of two-geographical jurisdictions that make autonomous, independent decisions, cooperatively or non-cooperatively, but populations interact in the same environment through travel. Though decisions are made independently, because of travel between jurisdictions, the actions of one jurisdiction can influence the epidemic in the other jurisdiction. This scenario would especially be of interest for a jurisdiction that makes the optimal decisions but has travels coming from a jurisdiction with bad decisions. While travel between jurisdictions would be favorable for the economy, it could diminish the impact of its optimal actions. Therefore, taking the perspective of a jurisdiction that makes the optimal decision, we evaluate under travel when actions of another jurisdiction significantly add to its disease and economic burdens. This would help inform when border closures would need to be part of an optimal lockdown strategy. And subsequently, whether decision-making control should be given to individual jurisdictions (say county-level or state-level) or a common entity (such as state if jurisdictions are counties, and federal if jurisdictions are states). In this study, we assume that both jurisdictions start an outbreak at the same time, thus our results are limited to this scope.

In highlighting the dynamic nature of infectious diseases, we underscore that a single policy would not suffice for all disease types. Thus, our work provides a robust framework and a powerful tool for decision analysis rather than a one-size-fits-all solution. The significance and potential applicability of this model have been further emphasized through comprehensive sensitivity analyses.

The rest of the paper is organized as follows. Section 2 presents the methodology, including the simulation model, MDP formulation, and RL. In section 3, we discuss the scenarios we analyzed in detail. Section 4 presents the results, Section 4.1 includes sensitivity anaylysis, and finally, in Section 5, we conclude the study with a discussion.

2. Methodology

Our model framework includes a compartmental simulation model that simulates the epidemic spread discussed in Section 2.1 integrated with a Markov decision process (MDP) optimization framework discussed in Section 2.2 and solved using deep Q-network (DQN) discussed in Section 2.3.

2.1. Simulation model

We developed a susceptible(S)-exposed(E)-infected(I)-recovered(R)-dead(D) (SEIRD) compartmental model based on Kermack and McKendrick [19] for simulating epidemic projections over time (Figure 1). An individual starts in compartment S, and upon contracting the disease moves to compartment E. A person in compartment E is in the incubation phase of the disease (for a duration of $1/\alpha$ days) and thus cannot transmit the disease. A person moves from compartment E to compartment I, the transmissible phase of the infection. A person in compartment I either recovers, i.e., moves to R with rate γ per day, or succumbs to disease, i.e., moves to D with rate θ per day.
Let

S be the number of Susceptible,
E be the number of Exposed,

I be the number of Infectious,
R be the number of Recovered,
D be the number of Dead,
N be total population,
β: transmission rate from susceptible to infected ($\beta = pc$ where p is the probability of transmission per susceptible-infected contact and $c =$ number of contacts per person), α: is the inverse of the average incubation period in days, γ: rate of recovery per day, and
θ: rate of disease-related mortality per day.

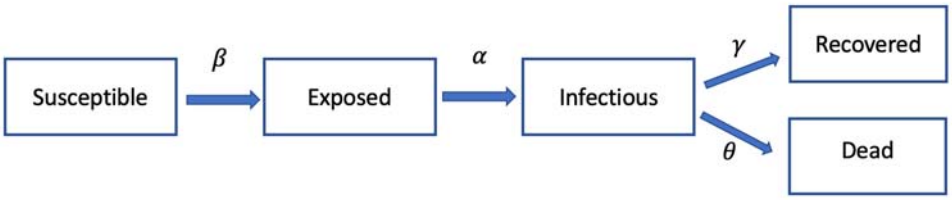

Figure 1. SEIRD flow diagram for infectious diseases.

Given the short duration of the disease, we evaluate over a short analytic period of 400 days, assuming no births or natural deaths, and thus, the population size remains constant over time ($N = S(t) + E(t) + I(t) + R(t) + D(t)$). The differential equation governing the dynamics of the disease can be written as follows:

$$\begin{aligned} \frac{dS}{dt} &= -\beta S\frac{I}{N} & S(0) &= S_0 \geq 0 \\ \frac{dE}{dt} &= \beta S\frac{I}{N} - \alpha E & E(0) &= E_0 \geq 0 \\ \frac{dI}{dt} &= \alpha E - \gamma I & I(0) &= I_0 \geq 0 \\ \frac{dR}{dt} &= \gamma I & R(0) &= R_0 \geq 0 \\ \frac{dD}{dt} &= \theta I & D(0) &= D_0 \geq 0 \end{aligned} \tag{1}$$

Population Mixing: To study the impact of travel on epidemic projections, we modified the standard SEIRD equations to include travel between two jurisdictions (jurisdiction A and jurisdiction B).
Let
r_{AB} be the travel rate from jurisdiction A to jurisdiction B,
r_{BA} be the travel rate from jurisdiction B to jurisdiction A, and
I_B be the number of infectious people in jurisdiction B.
Then the SEIRD model can be modified to include population mixing as follows:

$$\begin{aligned} \frac{dS_A}{dt} &= -\beta S_A(1-r_{AB})\left[\frac{(1-r_{AB})(I_A)+(r_{BA})(I_B)}{(1-r_{AB})N_A+(r_{BA})N_B}\right] - \beta S_A(r_{AB})\left[\frac{(r_{AB})(I_A)+(1-r_{BA})(I_B)}{(r_{AB})N_A+(1-r_{BA})N_B}\right] \\ \frac{dE_A}{dt} &= \beta S_A(1-r_{AB})\left[\frac{(1-r_{AB})(I_A)+(r_{BA})(I_B)}{(1-r_{AB})N_i+(r_{BA})N_B}\right] + \beta S_A(r_{AB})\left[\frac{(r_{AB})(I_A)+(1-r_{BA})(I_B)}{(r_{AB})N_A+(1-r_{BA})N_B}\right] - \alpha(E_A) \\ \frac{dI_A}{dt} &= \alpha(E_A) - \gamma I_A \\ \frac{dR_A}{dt} &= \gamma I_A \end{aligned} \tag{2}$$

$$\frac{dD_A}{dt} = \theta I_A.$$

Note that setting $r_{AB} = r_{BA} = 0$ in (2) results in (1), and hence the single jurisdiction model is a special case of the two-jurisdiction model. For empirical analyses, we used epidemiology data from the SARS-Cov2 alpha variant (Table 1).

Table 1. Parameters of the simulation model.

Parameter	Value	Description
β	0.4482	Transmission rate [20]
α	0.1923	1/interval in days for incubation (incubation period ~ 5.2 days) [21]
γ	0.1724	1/interval in days from infected to removal (infectious period ~ 5.8) [20,21]
θ	0.017	The mortality rate due to infections (in scenario 1 to 5, $\theta = 0$) [22]

We utilized a compartmental model which could be substituted with any simulation environment, such as agent-based modeling, depending on the nature of the disease spread. While compartmental models are usually more apt for rapidly spreading diseases, allowing for heterogeneity by partitioning compartments, agent-based models can be more suitable for slower spreading diseases, where contact structures play a significant role. However, it's important to note that our RL algorithm can be applied in either of these environments, as demonstrated in our previous paper [23].

2.2. Markov decision process

We formulate the question of whether a lockdown is necessary, and if so, when it should be initiated, to what level (proportion lockdown), and how this should change over time as an MDP, as follows. We define the pandemic state as a multivariate parameter $X = \left[\frac{S_A}{N_A}, \frac{E_A}{N_A}, \frac{I_A}{N_A}, \frac{R_A}{N_A}, \frac{D_A}{N_A}\right], X \in \mathbb{R}^5$, where $\frac{S_A}{N_A}, \frac{E_A}{N_A}, \frac{I_A}{N_A}, \frac{R_A}{N_A}$, and $\frac{D_A}{N_A}$ are the proportion of the jurisdiction A population in the S, E, I, R, and D compartment, respectively, and add to 1.

Then, using the standard form, we can define the MDP as a 5-tuple $\{\Omega, \mathcal{A}, P_a, R_a, \gamma\}$, where,

- Ω is the state space, a set of all possible states of the pandemic, $X \epsilon \Omega$,
- $\mathcal{A}$ is the action space, a set of all possible actions, here choices of lockdown, $a \epsilon \mathcal{A}$,
- P_a is the one-step transition probability matrix from one state of pandemic to another under action a (where $P_a(x'|a,x)$ is the transition probability from state x to x' under action a),
- $\mathcal{R}_a$is a reward matrix, with each element, $\mathcal{R}_a(x'|a,x)$, the immediate reward of transitioning from state x to x' under action a, and
- γ is the discount factor.

Given the system is in state $x_0 \in \Omega$ at time of implementation of decision, the problem is to solve for the optimal policy ($\boldsymbol{d}(x_0)$) using the following objective function to maximize the total expected reward over the analytic period T (for numerical analyses we assumed $T = 400$):

$$\max_{[d_1,..,d_T]\epsilon\mathcal{A}^T} \mathbb{E}\left[\sum_{t=1}^{T} \gamma \mathcal{R}_{a=d_t}(x'|a,x)\right]$$

$$\boldsymbol{d}(\boldsymbol{s}) = arg \max_{[d_1,..,d_T]\epsilon\mathcal{A}^T} \mathbb{E}\left[\sum_{t=1}^{T} \gamma \mathcal{R}_{a=d_t}(x'|a,x)\right] \quad (3)$$

We next discuss the formulation of the 5-tuple $\{\Omega, \mathcal{A}, P_a, \mathcal{R}_a, \gamma\}$:

State space: We formulate the state space as $\Omega = [\frac{S_A}{N_A}, \frac{E_A}{N_A}, \frac{I_A}{N_A}, \frac{R_A}{N_A}, \frac{D_A}{N_A}]$, a continuous state space where each element of the state space can get a value between 0 and 1, such that at each time step, $\frac{S_A}{N_A} + \frac{E_A}{N_A} + \frac{I_A}{N_A} + \frac{R_A}{N_A} + \frac{D_A}{N_A} = 1$.

Action space: We formulated the action space ($\mathcal{A}$) as a finite discrete set of interventions, $\mathcal{A} = [a_1 = 75\%, a_2 = 50\%, a_3 = 25\%, a_4 = 0\%]$, corresponding to a contact rate reduction of 75, 50, 25 and 0%, respectively, a factor multiplied to the transmission rate (β) in (1) and (2). For these numerical analyses, to make it representative of the COVID-19 epidemic, we assumed contact reductions are achieved through lockdowns. We assumed about 25% of the U.S. population are essential personnel [24] (34% of adults reported as essential personnel, and 78% of the population are adults) and thus the strictest lockdown, a_1, corresponds to a 75% reduction in contact rate. Value of action a_4 was selected to represent no-lockdowns, and values of actions a_2 and a_3 were set at intermediate levels between a_1 and a_4.

Transition probabilities: As generating the transition probability for every possible transition is infeasible, we use our SEIRD simulation model discussed earlier to simulate each action and keep track of each transition in the model.

Immediate rewards: Immediate reward ($\mathcal{R}_a(x)$) corresponds to the per time step reward (benefits – costs) achieved by implementing an *action* when the system is in *state* x. We evaluated immediate reward $\mathcal{R}_a(x)$ under two objective functions:

- 2-term objective function: The objective is to minimize economic burden and hospital capacity violation. This objective function would be most suitable for diseases that have a high risk of hospitalization, but minimal risk of mortality.
- 3-term objective function: The objective is to minimize economic burden, hospital capacity violation, and minimize mortalities. This objective function would be most suitable for diseases with high risk of hospitalizations and mortality.

Mathematically, we formulated the immediate reward $\mathcal{R}_a(x)$:

$$\mathcal{R}_a(x) = f_e(a) - f_h\big(I_{x,A}\big) - \eta\big[\theta I_{x,A} C_l\big] \tag{4}$$

where, setting $\eta = \begin{cases} 0 \text{ results in } 2-\text{term objective function} \\ 1 \text{ results in } 3-\text{term objective function'} \end{cases}$

$f_e(a)$ is the per day monetary benefit of implementing action a, $f_h\big(I_{x,A}\big)$ is the per day cost of exceeding hospital capacity in jurisdiction A, when there are $I_{x,A}$ number of infected persons, θ is the mortality rate, and thus $\theta I_{x,A}$ is the number of daily deaths in jurisdiction A when there are $I_{x,A}$ number of infected persons, and C_l is the per person mortality cost.

We modeled the monetary benefit ($f_e(a)$) as the economic benefit,

$$f_e(a) = \tau(a) M, \tag{5}$$

where, $\tau(a)$ is the monetary reduction in the economy upon implementation of action a and M is the per day monetary value generated by the economy in a no-lockdown scenario. Here, we assumed $M = 1e + 11$, and set $\tau(a_1) = 0.4$, $\tau(a_2) = 0.6$, $\tau(a_3) = 0.8$, and $\tau(a_4) = 1$. Per day monetary value of M is assumed based on US gross domestic product (GDP) per capita multiplied by US population in 2020 [24].

We assumed that for every 1000 inhabitants, there is 1.5 hospital beds available (we used data in the state of Utah which has the lowest number of beds per capita among US sates [25]) ($N_{beds} = \frac{1.5 N_A}{1000}$) and that 5% of infected people at each timestep are hospitalized [20,22], and modeled the per day cost of exceeding hospital capacity ($f_h\big(I_{x,A}\big)$) as

$$f_h(I_{x,A}) = \begin{cases} 1e+11 & \text{if } 5\% I_{x,A} \geq N_{beds} \\ 0 & otherwise \end{cases} \quad (6)$$

We assumed mortality rate is 0.017 corresponding to the SARS-Cov2 virus [22], and the cost per mortality (C_l) as $1e+10$.

2.3. Deep reinforcement learning

We solve for the optimal sequence, level, and time of initiation of lockdowns for the control of COVID-19 type new infectious disease outbreaks, formulated above as an MDP, using DQN. We solve for this under varying scenarios (see Section 3). DQN is a deep reinforcement learning algorithm suitable for continuous state and discrete action spaces [5]. Conceptually, the algorithm works as follows. At each time step, based on the state of the pandemic, i.e., values for $[\frac{S_A}{N_A}, \frac{E_A}{N_A}, \frac{I_A}{N_A}, \frac{R_A}{N_A}, \frac{D_A}{N_A}]$, the algorithm determines what action to take, feeds it to the simulation model to calculate the immediate reward of taking that action at that particular state. This process is repeated for multiple iterations, and at every iteration, through training of a neural network, the algorithm is learning to take better actions, such that, under the proper neural network architecture and hyper-parameters, the algorithm eventually learns to identify the decision that maximizes the objective function defined in (3). We developed the model using the stable_baselines library in Python [25]. The details of the algorithm are presented in Supplementary Section S.1.

DQN configuration and hyper-parameters: To approximate the Q-function, we used a deep learning network, a multi-layer perceptron with four layers that have 64, 128, 128, and 8 nodes, respectively. We use γ = 0.95 and a learning rate of 0.001 with buffer size 100000. The rest of the parameters are set as default by the stable_baselines DQN library [25]. We trained each scenario separately for different number of MDP iterations (referred to as episodes), each 100 times with different random seeds.

The initial state at the beginning of each episode is set to one person exposed for jurisdiction A and two persons exposed for jurisdiction B, and rest of the population are susceptible. Each episode is 400 days, and at the end of each episode, the model is reset to the initial state. We trained the model for different episodes from 2500 to 25000 (corresponding to 1 to 10 M time-steps). At the end of the training, we identify the optimal solution as the best among all the trained models, i.e., the model with the highest expected total reward (defined in (3)).

Similar to many optimization problems, DQN does not guarantee reaching the optimal solution, however, by sufficiently exploring the solution space, the chance of finding an optimal solution could be increased. Therefore, for each scenario (Section 3), we generated 100 different runs of the algorithm, each with a different random seed, and identifying an optimal solution under each. Similar optimal solutions in multiple runs would also suggest higher chance of optimality.

3. Analyses scenarios

We analyzed seven scenarios. Scenario 1 to 5 correspond to the 2-term objective (that considers impact of decisions on economy and hospital capacity violation), while scenarios 6 and 7 correspond to the 3-term objective (that consider the impact of decisions on economy, hospital capacity violation, and disease related mortality). Scenarios 1 and 6 correspond to a single jurisdiction while the rest of the scenarios correspond to two-jurisdictions with different travel rates. In the two-jurisdiction scenarios, decisions are made independently, and we consider two distinct behaviors among them. In scenarios 2 and 3, jurisdiction A implements the optimal policy but jurisdiction B does not implement

any intervention (non-cooperative behavior), while in scenario 4 and 5, jurisdiction B follows the exact same policy as A (cooperative behavior). However, note that, even in Scenarios 4 and 5, just as in Scenario 1 to 3, the formulation of the DQN focused only on the epidemic state in jurisdiction A. Thus, the DQN here was still a single-agent RL but evaluated in the context of two interacting jurisdictions making autonomous independent decisions. We further expanded these scenarios into sub-scenarios by examining the impact of delay in initiation of optimal policy, i.e., delaying initiation of optimal policy until day 30, 45, 60, 75, 90, 95, 100, 105, and 110 such that each corresponds to different prevalence upon initiation of optimal policy.

Intuitively, if the optimal policy is a lock-down, the more the delay in initiation of lockdown, the more the epidemic burden, but less of an economic burden. On the other hand, if the optimal policy is no-lockdown, it is equivalent to doing nothing, and so a delay in implementing optimal policy would not have any consequences until it reaches a time where the optimal policy shifts to a lockdown. Thus, the model technically considers the impact of delay and the tradeoff between economy and epidemic burden into its evaluation. Hence, the resulting optimal policy would also hold the answer to when a shutdown should be initiated. Besides, in the case of open borders, the optimal policy also changes based on the epidemic in the jurisdictions that the population interacts with through travel. However, the results would depend on how much weight (costs) is given to each objective function component. These costs associated with hospital capacity and lockdowns are likely to be subjective. For example, a jurisdiction where a significant fraction of jobs can seamlessly transition to remote work (e.g., IT) may differently weigh each of the four lockdown options (e.g., fewer days but maximum lockdown-level) compared to a jurisdiction where a large fraction of the jobs require physical presence (e.g., manufacturing) (e.g., extend days of lockdown at low lockdown-levels on each day). On the other hand, an infectious disease that is not deadly may be weighed lower for disease burden (hospital capacity as proxy) than a more deadly disease. Therefore, we made 'time to initiate' the optimal policy as an exogenous variable and evaluated multiple values. Details of the scenarios are discussed in Table 2.

For each scenario, 1 to 7, we present the following metrics: the frequency of occurrence of each action over a 400-day period, the total number of days hospitalizations exceeded hospital capacity (which we will refer to as "hospital capacity violation"), number of hospitalizations, and additionally for Scenarios 6 and 7, the number of deaths.

We present the "initiation of optimal policy" in days, which is how it was modeled, but also present the corresponding disease states, specifically, the observed prevalence and the actual prevalence. We define observed prevalence as the cumulative number of reported cases, tracked as part of disease surveillance, and expressed as a percentage of the total population. We define actual prevalence as the cumulative number of infected cases, i.e., it additionally includes those cases that are not yet reported and expressed as a percentage of the total population. Therefore, while the "initiation of optimal policy" was modeled in days, the corresponding observed prevalence is more relevant and trackable from a public health perspective. In the case of the SARS-CoV2 virus, persons in the "*exposed*" compartment are asymptomatic, and only show symptoms when they transition to the "*infectious*" compartment. Therefore, we made a simplifying assumption that the observed prevalence includes all cases except those in the *exposed* compartment (i.e., includes infectious + recovered + death compartments), while the actual prevalence also includes the *exposed* compartment.

Note that, while all scenarios were modeled with the same time-points for 'delay in initiation', the epidemic projections under the different travel rates would be different and thus the corresponding values of observed prevalence and actual prevalence would vary by scenarios. For instance, 90 days of delay in scenario 1 corresponds to an observed prevalence of 1.35% and the actual prevalence of 2.13%, while the same days of delay in scenario 3 correspond to an observed

prevalence of 1.9% and an actual prevalence of 3%. Therefore, we represent each sub-scenario, as [delay in initiation (in days), observed prevalence, and actual prevalence].

Table 2. Summary of the scenarios studied.

Scenario	Objective function	Number of jurisdictions	Policy	Travel from B to A	Initiation of optimal policy (days)
Scenario 1	2-term	Single jurisdiction, A	A optimal policy	Not applicable	30, 60, 75, 90, 95, 100, 105,110
Scenario 2	2-term	Two jurisdictions, A and B	A optimal policy, B no intervention	5%	30, 60, …, 110
Scenario 3	2-term	Two jurisdictions	A optimal policy, B no intervention	10%	30, 60, …, 110
Scenario 4	2-term	Two jurisdictions	A optimal policy, B optimal policy	5%	30, 60, …, 110
Scenario 5	2-term	Two jurisdictions	A optimal policy, B optimal policy	10%	30, 60, …, 110
Scenario 6	3-term	Single jurisdiction	A optimal policy	Not applicable	30, 60, …, 110
Scenario 7	3-term	Two jurisdictions	A optimal policy, B no intervention	10%	30, 60, …, 110

4. Results

In all scenarios, as expected from the highly virulent SARS-CoV2 virus, the optimal scenarios involved some lockdown until a majority of the population became infected or lasted for the entire simulation duration. In the 2-objective function scenarios (Scenarios 1 to 5), the optimal lockdown strategy helped avoid hospital capacity violations while minimizing the economic burden from lockdowns by taking the least stringent lockdown. However, the optimal policy was to end lockdown only after a majority of the population became infected and reached herd-immunity levels. In the 3-objective function scenarios (Scenarios 6 and 7), the optimal lockdown strategy helped avoid hospital capacity violations, minimize infected cases and deaths while minimizing the economic burden from lockdowns by taking the least stringent lockdown. However, the optimal strategy here was to continue the optimal pattern of lockdowns for the remaining duration of the simulation, suggesting that until a vaccine becomes available, there is a chance that the infection would spread. We discuss these results in more detail below.

With only one jurisdiction (Scenario 1), the optimal strategy was to initiate lockdown if the observed prevalence (proportion of the population infected) reached 2.3% (which corresponded to the actual prevalence of 3.6%). This can be seen in Figure 2 (first row), scenarios where lockdown initiated at the observed prevalence of 2.3% or below (corresponding to up to 95 days from time of first case) had least lockdown and similar outcome of zero hospital capacity violations. Over the duration of 400 days, this optimal policy consisted of lockdown at 50% for 62 days and lockdown at 25% for 46 days. Under this policy, lockdowns could be fully lifted on day 209. In the optimal strategy, the number hospitalized per day never exceeded hospital capacity, i.e., zero days of hospital capacity violation. As expected from including only economy and hospital capacity in the objective function, given the high

infectiousness of the virus and absence of other interventions, about 79% of the population were infected over the duration of the pandemic Figure 3 (first row).

Delaying implementation of optimal policy in Scenario 1, i.e., initiating lockdown after observed prevalence exceeded 2.3%, led to more prolonged or more stringent lockdowns and/or hospital capacity violations (Figure 2 first row). For example, delaying to until 3.8% observed prevalence led to 73 days of 50% shutdown, 27 days of 25% shutdown, and zero days of hospital capacity violation. Delaying to 6.4% observed prevalence led to 6 days of 75% shutdown, 52 days of 50% shutdown, 36 days of 25% shutdown, and five days of hospital capacity violation. Delaying to until 10.46% observed prevalence led to 17 days of 75% shutdown, followed by 34 days of 50% shutdown, 41 days of 25% shutdown, and 16 days of hospital capacity violation. While the 1.35% observed prevalence occurred on day 90, the observed prevalence of 2.3%, 3.88%, 6.43%, and 10.46% occurred on days 95, 100, 105, and 110, suggesting that because of the high infectiousness of the virus, a few days of delay could lead to significantly worse disease and economic burdens.

When jurisdiction A interacted with jurisdiction B through travel, but jurisdiction B was non-cooperative and did not take the optimal decision as A (Scenarios 2 and 3 –with 5% and 10% travel, respectively), the optimal policy for A was to control for B's non-cooperative actions through more stringent lockdowns than in Scenario 1 (0% travel). Even with the lower 5% travel (Scenario 2– Figure 2 second row) and initiating lockdowns when observed prevalence was as low as 0.002% (30 days delay), unlike in Scenario 1 (Figure 2 first row), the optimal lockdown involved 28 days of maximum 75% lockdown.

In Scenario 2, the optimal lockdown strategy up until observed prevalence of 3.07% were similar with outcomes of zero days of hospital capacity violation. The optimal policy, over the period of 400 days, was lockdowns at the maximum-level of 75% for 37 days before transitioning to the less stringent 50% and 25% levels. Delayed implementation of optimal policy until the observed prevalence reached 5.17% led to the need for more stringent lockdowns (41 days of the maximum 75%, 20 days of 50%, and 42 days of 25%) to avoid hospital capacity violation. Delaying implementation of optimal policy to beyond observed prevalence of 5.17% led to a situation where hospital capacity violations could not be avoided (Figure 2 second row). For example, delaying until 8.54% observed prevalence led to 58 days of 75% shutdown, and 11 days of hospital capacity violation. Delaying to until 13.73% observed prevalence led to 47 days of 75% shutdown, and 24 days of hospital capacity violation.

In Scenario 3 (Figure 2 third row), the optimal policy was to initiate a lockdown no later than an observed prevalence of 5.52%. The optimal policy, over the period of 400 days, was lockdowns at the maximum level of 75% for 57 days, which resulted in zero days of hospital capacity violation. Delaying implementation of optimal policy to after observed prevalence exceeded 5.52%, led to higher hospital capacity violations (Figure 2 third row). For example, delaying until observed prevalence was 9.07% led to 24 days of 75% shutdown, followed by 45 days of 50% shutdown, and 14 days of hospital capacity violation. Delaying until observed prevalence was 14.48% led to 33 days of 75% shutdown, followed by 36 days of 25% shutdown and 26 days of hospital capacity violation.

When jurisdiction A interacted with B through travel but unlike the above scenarios, B was cooperative by taking optimal actions as A (Scenarios 4 and 5), the optimal policy was similar to that in Scenario 1 (single jurisdiction, 0% travel), suggesting that cooperative behavior would yield similar results as single jurisdiction, as expected. Note that, similarity in results between Scenarios 4, 5 and 1 suggests that, though the DQN was trained as a single-agent RL by considering only the state space of jurisdiction A, this is a sufficient method here as we assumed that both jurisdictions start the epidemic at the same time.

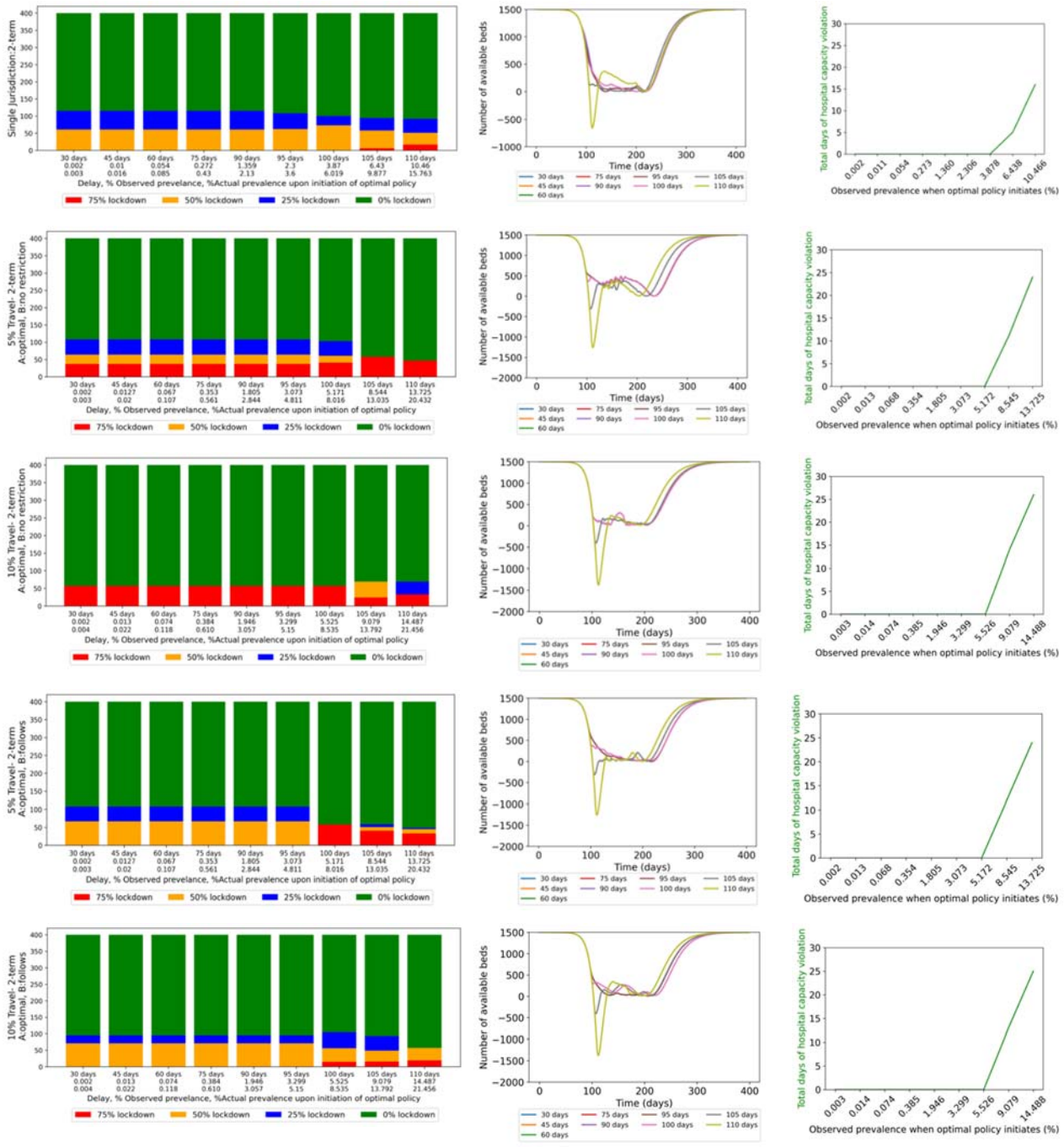

Figure 2. 2-term objective function models for scenarios 1, 2, 3, 4, and 5. Left plots: Bar plots of frequency of occurrence of each action (75% (red), 50% (yellow), 25% (blue), and 0% (red) lockdown) over 400 days for different delay (x-axis) in initiation of optimal policy [delay in days, observed prevalence, and actual prevalence]. Middle plots: Number of available hospital beds (y-axis) against time (x-axis) under different delays in initiation of optimal policy. Right plots: Total number of days hospital capacity is violated (y-axis) against observed prevalence at time of initiation of optimal policy (x-axis).

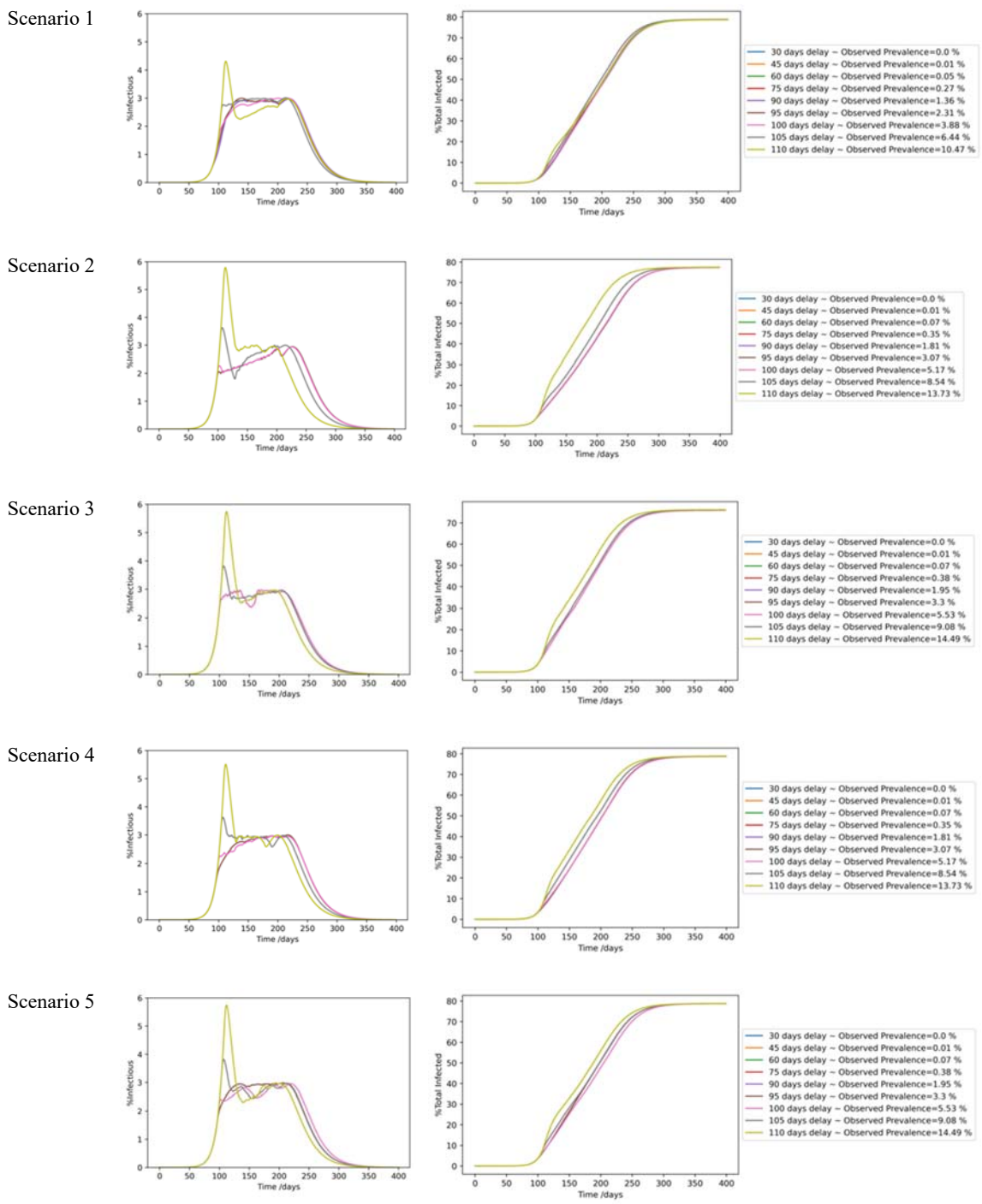

Figure 3. Percentage infectious among total population vs time for different delays in initiation of the optimal policy (left plots) and corresponding impact on percentage total infected over time (right plots) for scenarios 1, 2, 3, 4, and 5.

In summary, results from the above 2-objective function scenarios suggest that deviating from the optimal policy through delays in initiating the optimal policy or through non-cooperative behavior by an outside but interacting jurisdiction (B in this case) would require more stringent lockdowns (red bar) to avoid hospital capacity violations.

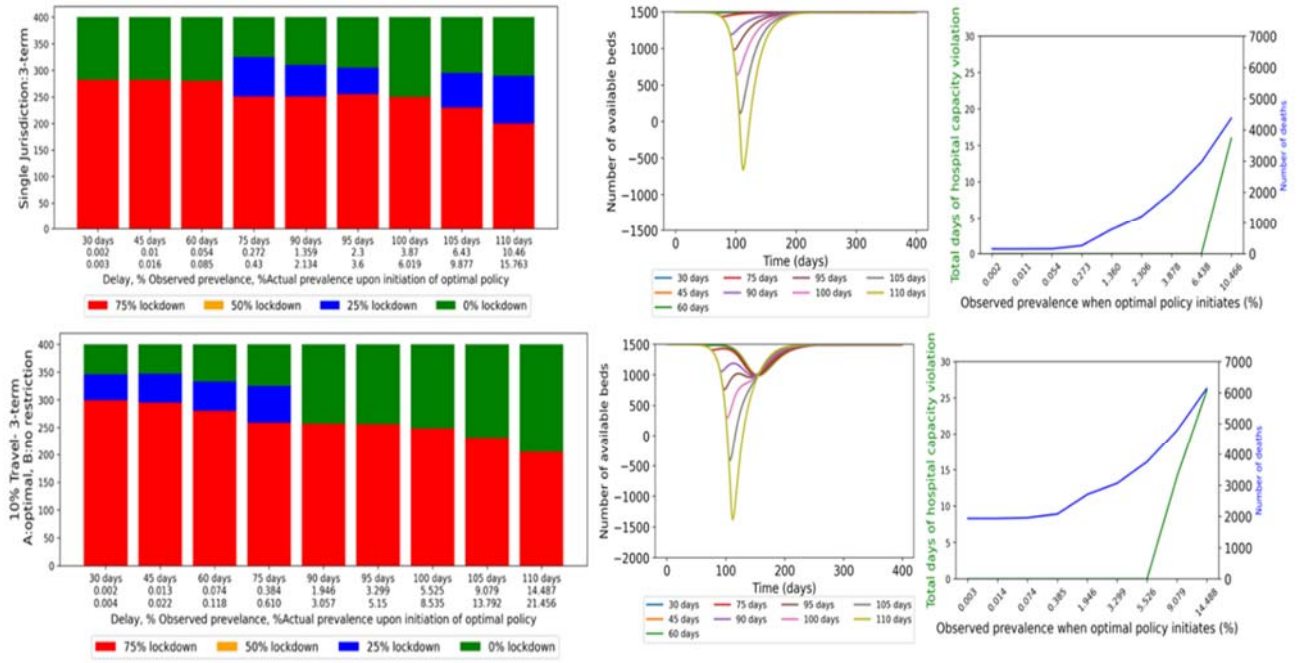

Figure 4. 3-term objective function models for scenarios 6 and 7. Left plots: Bar plots of frequency of occurrences of each action (75% (red), 50% (yellow), 25% (blue), and 0% (red) lockdown) over 400 days for different delays (x-axis) in initiation of optimal policy]delays in days, observed prevalence, and actual prevalence]. Middle plots: Number of available hospital beds (y-axis) against time (x-axis) under different delays in initiation of optimal policy. Right plots: Total number of days hospital capacity is violated (y-axis) against observed prevalence at time of initiation of optimal policy (x-axis).

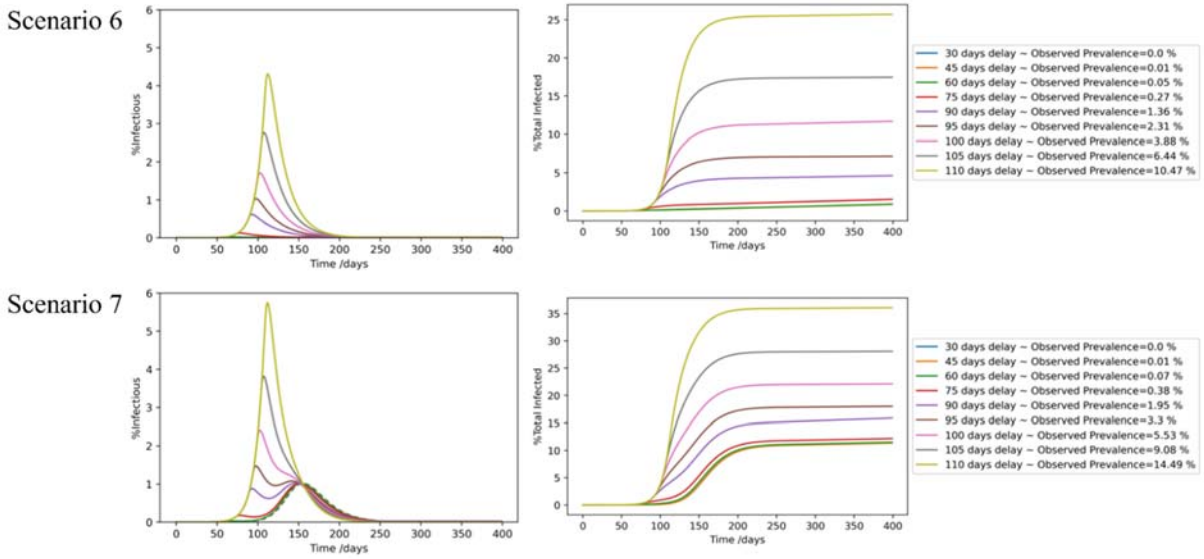

Figure 5. Percentage infectious among total population vs time for different delays in initiation of the optimal policy (left plots) and corresponding impact on percentage total infected over time (right plots) for scenarios 6 and 7.

With the 3-objective function, and only one jurisdiction (Scenario 6), the optimal policy was to initiate lockdown when observed prevalence was 0.01% (Figure 4 first row). Under this, the optimal lockdown policy continued for the remaining duration of the simulation in order to reduce cases and keep deaths at zero. This suggests that until pharmaceutical options are available, preventing highly transmissible diseases such as COVID-19 would require some level of physical distancing between contacts. Delaying the initiation of the optimal policy generated multiple deaths even though higher number of lockdowns were initiated to control for the delays. Delaying implementation of an optimal strategy to prevalence 10.46% (which occurred on day 110 from the first infection) resulted in 4374 deaths, and 16 hospital capacity violations (Figure 4 first row, and Supplementary Table S2).

With the 3-objective function, when jurisdiction A was interacting with B through travel, but jurisdiction B was not implementing any interventions (Scenario 7), the optimal strategy for A to control for the non-cooperative behavior of B were a greater number of days and more stringent lockdowns. Under this, the optimal policy over the 400 days was lockdown at the highest-level of 75% for 299 days and at 25% for an additional 47 days (Figure 4 row 2). This optimal policy resulted in zero days of hospital capacity violation but 1935 deaths (Figure 4 row 2). Delaying implementation of the optimal policy until observed prevalence reached 8.5%, led to a situation where the epidemic burden had already created sufficient deaths that lockdowns had a lesser impact and could only be implemented to reduce future deaths than to prevent deaths. The optimal policy in this case was 231 days of the highest-level of 75% lockdown and resulted in 4775 deaths and 14 days of hospital capacity violation.

Comparing results between 2-objecive and 3-objectve functions: In the 2-term objective function, as the objective was to only minimize economic burden and hospital capacity violations, the cumulative prevalence reached up to 80%, (Figure 3) i.e., the main outcome was that it reduced daily cases sufficient enough to keep hospitalizations below hospital capacity. In the 3-objective function, as the objective additionally minimized deaths, even in the worst-case scenario the cumulative prevalence reached about 35% (Figure 5). However, a key consequence of this was that, while in the 2-objective function lockdowns could be lifted within the timeline of the simulation, in the 3-objective function lockdowns continued over the full duration of the simulation. This suggests the need for continuing shutdowns until the availability of pharmaceutical interventions such as treatment to prevent deaths or vaccines to prevent transmissions.

Details of optimal policy of each sub-scenarios of 2-objective and 3-objective are presented in Supplementary Table S1.

4.1. Sensitivity analysis

We conducted to analysis to show how sensitive our results are to the selected transmission rate (β, crucial factor in modeling the spread of infectious diseases): a) widely varying transmission rate values b) -8.5 to + 9% change around COVID-specific values. The first to represent different virus strains/ viruses and the second to represent uncertainty in values for a fixed virus strain.

We tested the sensitivity of our results for single jurisdiction (Scenario 1) to the transmission rate β in Table 1 using the learned model. The transmission rate was varied from 0.3 to 0.5 in increments of 0.1. Additionally, a more fine-grained variation in transmission rates compared to the baseline transmission rate ($\beta = 0.448$) was also tested ($\beta = 0.41, 0.42, 0.43, 0.45, 0.46, 0.47, 0.48, 0.49$).

Results are robust within the values of uncertainty range (-4.06% and $+ 0.401\%$, values of uncertainty range). However, as expected, if there are different viruses, or virus strains evolve over time, as was the case with COVID, then the analyses should be redone to identify a policy specific to that strain.

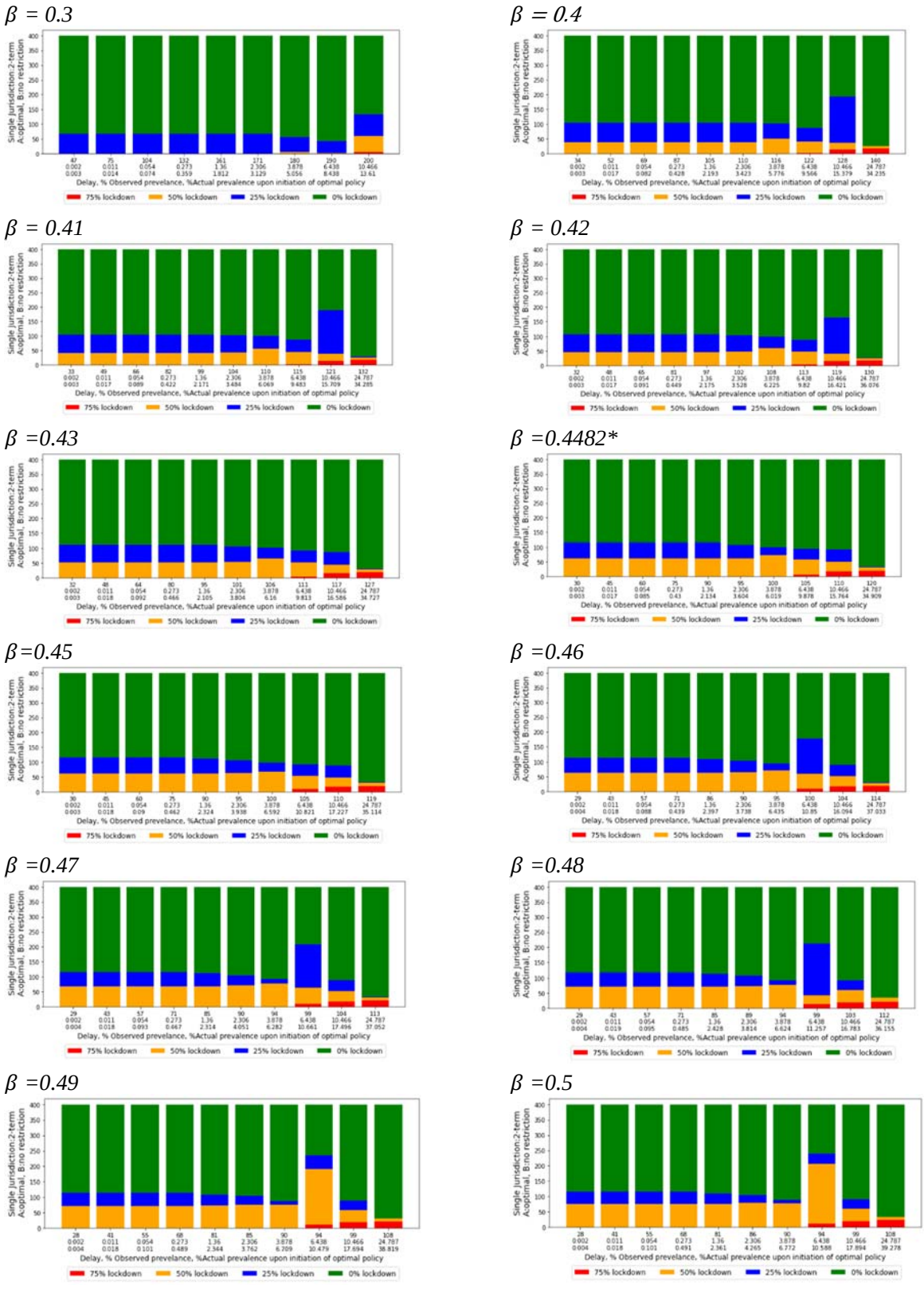

Figure 6. Sensitivity analysis on impact of transmission rate (β on optimal policy for single jurisdiction (Scenario 1). % Observed prevalence upon initiation of optimal policy is kept constant as the point of references for comparing different transmission rates. This value is translated into different % actual prevalence and delay (line 1 and 3 of x-axis). *: Basecase value for β

In the plots depicted below, the observed prevalence serves as a reference point for assessing the impact of delayed policy implementation. It is evident that the lower the transmission rate, the less restrictive the lockdown measures can be. This relationship highlights the importance of considering both observed prevalence and transmission rates when determining the most effective strategies to control the spread of infectious diseases.

The sensitivity analysis aimed to evaluate how changes in the transmission rate influenced the optimal policy. The results highlighted the following points:

Optimal Policy Sensitivity: The optimal policy in general was found to be sensitive to variations in the transmission rate, however when more fine-grained transmission rates were tested, we observed that optimal policies for $\beta = 0.43$ and 0.5 (Figure 6, third and fourth rows) are more consistent with the baseline value ($\beta = 0.448$). But the recommended optimal policy deviates from baseline for transmission rates smaller or larger than the baseline value. As a result, the model is robust to uncertainty in transmission rate up to -4.06% and $+0.401\%$, but higher/ lower uncertainty in transmission rate requires a new RL learning process to find the optimal policy and to devise an effective strategy to control the spread of the disease.

Deviation from the Paper's Value: The results also showed that as the tested transmission rate deviated further from the value specified in the paper (0.448), the optimal policy changed more significantly. This highlights the fact that epidemics characterized by distinct parameters necessitate models trained across a corresponding spectrum of values for optimal performance. The specificities of the disease parameters, coupled with the non-linearity of disease progression, can result in drastically differing ranges of robustness for the learned models. This finding particularly challenges policies that exclusively depend on observed prevalence for public health decision-making.

Testing fine-grained transmission rates allowed for a more nuanced understanding of how the optimal policy changed with varying transmission rates. This level of detail is essential for policymakers to consider when tailoring their strategies to specific contexts and situations.

To make the comparison with basecase, we fixed the observed prevalence (values in second row of x-axis Figure 2 left hand-side plot) as the point in time that policy makers delay the decisions.

5. Conclusions and discussion

We formulated the question of how to control epidemics such as COVID-19 in the absence of pharmaceutical interventions as a sequential decision-making problem formulated as a Markov decision process (MDP) and solved using Deep Q-network (DQN), a reinforcement learning algorithm. We propose a methodology that can help determine whether and when a lockdown is necessary, to what level, and how to phase out a lockdown which is a critical part of a pandemic preparedness plan. Furthermore, we evaluated these decisions in the context of two-geographical jurisdictions that make autonomous, independent decisions, cooperatively or non-cooperatively, but interact in the same environment through travel. We evaluated these decisions both under a 2-term objective function that minimized economic burden and hospital capacity violations, suitable for diseases with high-risk of hospitalizations but low risk of mortality, and a 3-term objective function that additionally minimized deaths. We used a SEIRD model to simulate the disease progression and incorporated the impact of travel in the formulation of the transmission rate.

In the case of a single jurisdiction, under a 2-term objective, the optimal time for initiation of lockdowns would be at about an observed prevalence of 3.87% and included lockdowns at a combination of 50 and 25% per day. Delaying decisions led to a higher number or more stringent lockdowns at the maximum levels of 75% per day in addition to a higher number of hospital capacity

violations. In the case of two-jurisdictions A and B interacting through travel, if jurisdiction B deviated from the optimal policy, jurisdiction A would have to implement more stringent lockdowns to compensate for the non-cooperative behavior of B, and if there was any delay in this implementation also face excess hospitalizations. This suggests that, even if jurisdictions make decisions independently, cooperation between jurisdictions could help minimize lockdowns and avoid border travel restrictions, thus minimizing overall economic burden. In the absence of such cooperation, the trade-offs for jurisdiction A to consider would be between more stringent lockdowns within its jurisdiction or border closures to remove the interactions with jurisdiction B. The results are intuitive, what the study contributes is a methodology that can be used by jurisdictions to evaluate a suitable policy, under such interactive environments, and the numerical analyses here serves as proof-of-concept for the method.

In the 2-objective function scenarios (Scenarios 1 to 5), the optimal lockdown strategy helped avoid hospital capacity violations while minimizing the economic burden from lockdowns by taking the least stringent lockdown. However, as expected from the high transmissibility of the virus, the optimal policy was to end lockdowns only after a majority of the population became infected and reached herd-immunity levels. In the 3-objective function scenarios (Scenarios 6 and 7), the optimal lockdown strategy helped avoid hospital capacity violations, minimized infected cases and deaths while minimizing the economic burden from lockdowns by taking the least stringent lockdown. However, the optimal strategy here was to continue the optimal pattern of lockdowns for the remaining duration of the simulation, suggesting that shutdowns would have to continue until a vaccine became available. Any deviations from this optimal policy generated more stringent lockdowns and/or higher cases of hospitalizations and deaths. This suggests that, in the absence of pharmaceutical interventions, some measures of physical distancing would be necessary to control the epidemic even if it creates economic burdens, as deviating from this would only increase future economic burdens.

Finally, we conducted sensitivity analysis on imoact of transmission rate on our results for single-jurisdiction scenario, including 1) widely varying transmission rate for different virus strains/ viruses and 2) small changes around COVID-19 transmission rate value to represent uncertainty in values for a fixed virus strain. Results are robust within the values of uncertainty range (-4.06% and +0.401%, values of uncertainty range). However, as expected, if there are different viruses, or virus strains evolve over time, as was the case with COVID, then the analyses should be redone to identify a policy specific to that strain.

Some of the limitations of our model are as follows. Motivated by the COVID-19 pandemic, for the numerical analyses, we assumed epidemiology staging and transmissibility of the SARS-CoV 2 virus. Thus, the specific results here are limited to diseases caused by viruses similar to that of SARS-CoV 2 type. The model will have to be reparametrized and evaluated for other diseases with vary epidemiology structures. In our model, the impact of lockdowns on the economy is scaled linearly, i.e., lockdown on any day has a similar impact on the economy's monetary value. This impact can be formulated as a non-linear function to consider the dynamical changes over time. We assumed that both jurisdictions start an outbreak at the same time, thus it was sufficient to train the DQN as a single-jurisdiction RL with both jurisdictions implementing the same policy (as evident from the similarity in results between Scenario 4, 5, and 1). Thus, our results are limited to this scope. For evaluating decisions between two jurisdictions that start the outbreak at different times leading to significantly different states of the epidemic at the time of decision-making, other methods such as multi-agent RL maybe more relevant. The compartmental model utilized in this study could be replaced with any other simulation environment and can be enhanced to include more heterogeneity by further dividing the compartments. Besides, improving the performance of DQN algorithm was outside of scope of this model, but can be explored in future research.

We utilized the Deep Q-Network (DQN), an off-the-shelf RL algorithm, which has shown a broad spectrum of applicability to a vast number of problems in the literature. Fine-tuning the parameters of this algorithm was beyond the scope of this work; however, many studies exist to address how to improve performance, reduce computational complexities, and hardware requirements, which can be further studied in future works [26,27].

Despite these limitations, we believe that the methodology presented here can help decision makers in formulating a pandemic preparedness plan for future infectious disease outbreaks. The results generated by the numerical analyses are intuitive, which support the feasibility of application of AI algorithms for such analyses, as typically, given the computational complexity of the algorithms and problem formulation, the feasibility is not always guaranteed [28]. This study provides a generalized framework that can be applied to any jurisdiction or infectious disease by adjusting the parameters accordingly, some examples are as follows. We interpreted the intervention options here to represent lockdowns and did not consider other options such as facemask use, self-isolation when infected, or 6 ft distancing. However, we modeled lockdowns by reducing transmission rate, assuming that the cost for that reduction represents economic loss. Interventions such as facemask use, self-isolation when infected, or 6 ft distancing are also modeled as reduction in transmission rates, but they may differ in governmental lockdowns in terms of the cost and impact, i.e., they may have a lesser impact on the economy (lower costs) but also achieve a smaller reduction in transmission rate. Therefore, the different levels of shutdowns and costs modeled here can also be interpreted as different types of interventions and the corresponding transmission rate, rewards, and costs informed specific to the setting. Design of the *immediate reward* is an essential step in RL models and can significantly change the optimal policy. Thus, this is a subjective metric that should be informed specific to the case under study. For example, a jurisdiction where a significant fraction of jobs can seamlessly transition to remote work (e.g., IT) may differently weigh each of the four lockdown options (e.g., fewer days but maximum lockdown-level) compared to a jurisdiction where a large fraction of the jobs require physical presence (e.g., manufacturing, or essential workers). On the other hand, those costs saved from preventing economic loss could instead be redirected to ensure safety of workers. Thus, the *immediate reward* function would be formulated to consider economic costs, epidemic costs, and costs for safety measures. This work offers a framework and a tool for decision analysis, with the significance of this aspect emphasized through our sensitivity analyses. These considerations not only highlight the value of our study but also indicate potential avenues for further research and development.

Use of AI tools declaration

The authors declare they have not used Artificial Intelligence (AI) tools in the creation of this article.

Acknowledgments

This material is based upon work supported by the National Science Foundation NSF 1915481. Any opinions, findings, and conclusions or recommendations expressed in this material are those of the author(s) and do not necessarily reflect the views of the National Science Foundation. Dr. Khatami was affiliated to UMass Amherst at the time of study.

Conflict of interest

All authors declare no conflicts of interest in this paper.

References

1. S. Thomson, E. C. Ip, COVID-19 emergency measures and the impending authoritarian pandemic, *J. Law Biosci.*, **7** (2020). 1–13. https://doi.org/10.1093/jlb/lsaa064
2. A. L. Bertozzi, E. Franco, G. Mohler, M. B. Short, D. Sledge, The challenges of modeling and forecasting the spread of COVID-19, *Proc. Natl. Acad. Sci. U.S.A.*, **117** (2020), 16732–16738. https://doi.org/10.1073/pnas.2006520117
3. T. Oraby, M. G. Tyshenko, J. C. Maldonado, K. Vatcheva, S. Elsaadany, W. Q. Alali, et al., Modeling the effect of lockdown timing as a COVID-19 control measure in countries with differing social contacts, *Sci. Rep.*, **11** (2021), 3354. https://doi.org/10.1038/s41598-021-82873-2
4. *State/Local Activity Dashboard*, 2021. Available from: https://www.multistate.us/issues/covid-19-policy-tracker
5. V. Mnih, K. Kavukcuoglu, D. Silver, A. Graves, I. Antonoglou, D. Wierstra, et al., Playing atari with deep reinforcement learning, preprint, arXiv: 1312.5602.
6. R. S. Sutton, A. G. Barto, Reinforcement learning: An introduction, in *Adaptive computation and machine learning series*, MIT Press, Massachusetts, 2018.
7. Y. Liang, M. C. Machado, E. Talvitie, M. Bowling, State of the art control of Atari games using shallow reinforcement learning, preprint, arXiv: 1512.01563.
8. B. R. Kiran, I. Sobh, V. Talpaert, P. Mannion, A. A. Al Sallab, S. Yogamani, *et al.*, Deep reinforcement learning for autonomous driving: A survey, *IEEE Trans. Intell. Transp. Syst.*, **23** (2022), 4909–4926. https://doi.org/10.1109/TITS.2021.3054625
9. X. Chen, S. Li, H. Li, S. Jiang, Y. Qi, L. Song, Generative adversarial user model for reinforcement learning based recommendation system, in *Proceedings of the 36th International Conference on Machine Learning*, **97** (2019), 1052–1061.
10. S. Zhou, X. Liu, Y. Xu, J. Guo, A deep Q-network (DQN) based path planning method for mobile robots, in *2018 IEEE International Conference on Information and Automation (ICIA)*, (2018), 366–371. https://doi.org/10.1109/ICInfA.2018.8812452
11. H. Luo, S. W. Li, J. Glass, Prototypical q networks for automatic conversational diagnosis and few-shot new disease adaption, preprint, arXiv:2005.11153.
12. L. Chen, Q. Gao, Application of deep reinforcement learning on automated stock trading, in *2019 IEEE 10th International Conference on Software Engineering and Service Science (ICSESS)*, (2019), 29–33. https://doi.org/10.1109/ICSESS47205.2019.9040728
13. C. Colas, B. Hejblum, S. Rouillon, R. Thiébaut, P. Y. Oudeyer, C. Moulin-Frier, *et al.*, EpidemiOptim: A toolbox for the optimization of control policies in epidemiological models, *J. Artif. Intell. Res.*, **71** (2021), 479–519. https://doi.org/10.1613/jair.1.12588
14. G. H. Kwak, L. Ling, P. Hui, Deep reinforcement learning approaches for global public health strategies for COVID-19 pandemic, *PLoS ONE*, **16** (2021). https://doi.org/10.1371/journal.pone.0251550
15. A. Gosavi, Simulation-based optimization: Parametric optimization techniques and reinforcement learning, in *Operations Research/Computer Science Interfaces Series*, Springer, 2015.
16. H. Khadilkar, T. Ganu, D. P. Seetharam, Optimising lockdown policies for epidemic control using reinforcement learning: An AI-driven control approach compatible with existing disease and network models, *Trans. Indian Natl. Acad. Eng.*, **5** (2020), 129–132. https://doi.org/10.1007/s41403-020-00129-3
17. V. Kompella, R. Capobianco, S. Jong, J. Browne, S. Fox, L. Meyers, *et al.*, Reinforcement learning for optimization of COVID-19 mitigation policies, preprint, arXiv: 2010.10560.

18. M. Arango, L. Pelov, COVID-19 pandemic cyclic lockdown optimization using reinforcement learning, preprint, arXiv: 2009.04647.
19. W. O. Kermack, A. G. McKendrick, A contribution to the mathematical theory of epidemics, *Proc. R. Soc. Lond. A*, **115** (1927), 700–721. https://doi.org/10.1098/rspa.1927.0118
20. L. Miralles-Pechuán, F. Jiménez, H. Ponce, L. Martínez-Villaseñor, A deep Q-learning/genetic algorithms based novel methodology for optimizing COVID-19 pandemic government actions, preprint, arXiv: 2005.07656.
21. T. M. Chen, J. Rui, Q. P. Wang, Z. Y. Zhao, J. A. Cui, L. Yin, A mathematical model for simulating the phase-based transmissibility of a novel coronavirus, *Infect. Dis. Poverty*, **9** (2020), 24. https://doi.org/10.1186/s40249-020-00640-3
22. Centers for Disease Control and Prevention, *COVID Data Tracker*, 2021. Available from: https://covid.cdc.gov/covid-data-tracker/#cases_casesper100k
23. S. N. Khatami, C. Gopalappa, A reinforcement learning model to inform optimal decision paths for HIV elimination, *Math. Biosci. Eng.*, **18** (2021), 7666–7684. https://doi.org/10.3934%2Fmbe.2021380
24. U.S. BUREAU OF LABOR STATISTICS, *TED: The Economics Daily image*, 2021. Available from: https://www.bls.gov/opub/ted/2021/107-5-million-private-sector-workers-in-pandemic-essential-industries-in-2019.htm
25. A. Hill, *Stable Baselines*, 2018. Available from: https://github.com/hill-a/stable-baselines
26. Z. Tang, L. Luo, B. Xie, Y. Zhu, R. Zhao, L. Bi, et al., Automatic sparse connectivity learning for neural networks, *IEEE Trans. Neural Netw. Learn. Syst.*, **2022** (2022). https://doi.org/10.1109/TNNLS.2022.3141665
27. J. Zheng, C. Lu, C. Hao, D. Chen, D. Guo, Improving the generalization ability of deep neural networks for cross-domain visual recognition, *IEEE Trans. Cogn. Dev. Syst.*, **13** (2021), 607–620. https://doi.org/10.1109/TCDS.2020.2965166
28. T. Hagendorff, K. Wezel, 15 challenges for AI: or what AI (currently) can't do, *AI Soc.*, **35** (2020), 355–365. https://doi.org/10.1007/s00146-019-00886-y